21st IAEA Fusion Energy Conference
Chengdu, China, 16 - 21 October, 2006

IAEA-CN-149/ EX/8-1

Super Dense Core Plasma due to Internal Diffusion Barrier in LHD

N. Ohyabu et al.

NIFS-842 Oct. 2006

Super Dense Core Plasma due to Internal Diffusion Barrier in LHD

N. Ohyabu 1), T. Morisaki 1), S. Masuzaki 1), R. Sakamoto 1), M. Kobayashi 1)
J. Miyazawa 1), M. Shoji 1), T. Akiyama 1), N. Ashikawa 1), M. Emoto 1), H .Funaba 1), P. Goncharov 1), M. Goto 1), J.H. Harris 2), Y. Hirooka 1), K.Ichiguchi 1) T. Ido 1), K. Itoh 1), H. Igami 1), K. Ikeda 1), S. Inagaki 1), H .Kasahara 1), T. Kobuchi 1), S. Kubo 1), R. Kumazawa 1), S. Morita 1) S. Muto 1), K. Nagaoka 1), N. Nakajima 1), Y. Nakamura 1), H. Nakanishi 1), K. Narihara 1) Y. Narushima 1), M. Nishiura 1), T. Notake 1), S. Ohdachi 1), N. Ohno 1), Y. Oka 1), M. Osakabe 1), T. Ozaki 1), B.J. Peterson 1), K. Saito 1), S. Sakakibara 1), R. Sanchez 2), H. Sanuki 1), K. Sato 1), T. Seki 1), A. Shimizu 1), H. Sugama 1), C. Suzuki 1), Y. Suzuki 1), Y. Takeiri 1), K. Tanaka 1), N. Tamura 1), K. Toi 1), T. Tokuzawa 1), S. Toda 1), K. Tsumori 1) I. Yamada 1), O. Yamagishi 1), M.Yokoyama 1), S. Yoshimura 1), Y. Yoshimura 1), M. Yoshinuma 1), K. Ida 1), T. Shimozuma 1), K.Y. Watanabe 1), Y. Nagayama 1), O. Kaneko 1), T. Mutoh 1), K. Kawahata 1), H. Yamada 1), A. Komori 1), S. Sudo 1), O. Motojima 1)

1) National Institute for Fusion Science, Toki, Gifu-ken, Japan
2) Oak Ridge national Laboratory, Ork Ridge, Tennessee,USA

e-mail contact of main author: ohyabu@LHD.nifs.ac.jp

Abstract A Super Dense Core (SDC) plasma operational regime has been discovered in the LID (Local Island divertor) discharges in LHD. The observed new confinement improvement regime is very attractive to future helical device. The SDC plasma has been established naturally by multiple pellet injection. A core region with density as high as 4.5×10^{20}m^{-3} and temperature of 0.85 keV is maintained by an Internal Diffusion Barrier (IDB). The density gradient in the IDB is very high and the time constant for the core density decay is about 1 s. The temperature gradient in the outer region beyond the IDB is similar to that in the outer region of the non-SDC discharge with similar plasma conditions. The size of the SDC increases with increasing β and increasing R_{ax} (vacuum magnetic axis). The maximum achieved stored energy is 1.1 MJ (at 10 MW of NBI power), achieving $n_o\tau_E T_o$ (fusion triple product) of ~ 4.6×10^{19} keVm^{-3}s. The density in the outer region, is kept low by pumping of the recycled particles by the LID, helping to raise the temperature gradient there and hence the core temperature.

1. Introduction

The LHD is a superconducting large helical device with a helical field with poloidal winding number l =2 and M = 10 toroidal field periods. The major radius of the magnetic axis, R_{ax} = 3.5-3.9 m, average plasma minor radius a = 0.5-0.6 m, and magnetic field B ≤ 3.0 T [1]. One of the major goals of the LHD program is demonstration of a diverted helical plasma with high performance, i.e., high $n_o\tau_E T_o$. A Local Island Divertor (LID)[3-6] has been installed for effective pumping of the recycled particles. It uses an n/m=1/1 resonant magnetic island to guide particle and heat fluxes to divertor plates. We attempted to explore a regime of confinement enhancement [2] with combination of pumping by the LID and core fueling by pellet injection and found a new attractive regime, which could extrapolate to the ignition in the helical device.

2. Observation of stable super dense core mode

We observed a stable **S**uper **D**ense **C**ore (**SDC**) mode in diverted discharges in the Large Helical Device (LHD) [7]. A **SDC** plasma develops naturally in LHD as a peaked, high density profile is generated by multiple pellet injections from the outside mid-plane as illustrated in Fig.1-a. The density and temperature profiles are shown in Fig. 1-b for a typical SDC discharge (R_{ax} (vacuum magnetic axis) = 3.75 m, B (magnetic field) = 2.64 T, P (absorbed NBI power) = 10 MW). They are measured by a Thomson diagnostic along R, the major radius, in the poloidal plane, where the plasma is horizontally elongated (Fig. 1-a). A core region with electron densities ~ 4.6×10^{20} m^{-3} and temperatures ~ 0.85 keV is maintained by an **I**nternal **D**iffusion **B**arrier (**IDB**) located at normalized minor radius $0.3 < \rho < 0.5$. The radial width of the IDB is ~ 0.1 m ($\Delta\rho \sim 0.2$). The density gradient outside the IDB is much lower than that in the IDB with n ~ 6×10^{19} m^{-3} at the last closed flux surface ($\rho = 1$). Unlike the tokamak ITB (internal transport barrier) discharges [8-10], the temperature gradient is very low in the IDB and core regions, possibly because the density becomes extremely large in LHD. The temperature gradient in the outer region is determined by anomalous thermal diffusivity. Low n_{edge} leads to higher edge ∇T_e and $T_e(0)$.

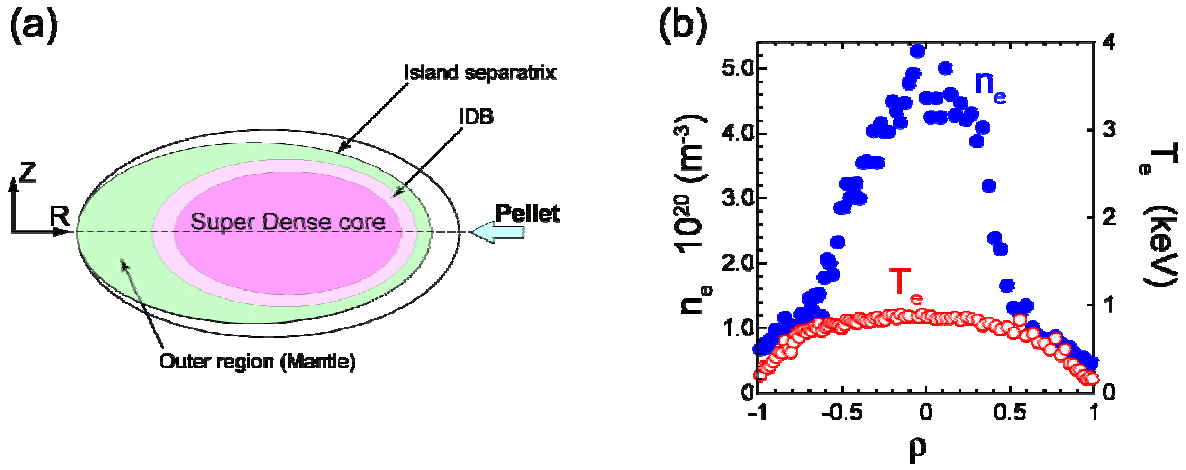

Fig. 1 (a) Illustration of an SDC plasma. (b) Density and temperature profiles of an SDC discharge with R_{ax} = 3.75m are depicted. P = 10 MW.

3. Time evolution of the SDC discharge

The production of the SDC begins with sequential injection of 6 or more pellets which penetrate beyond the magnetic axis and drive the formation of a strongly peaked density profile. We use 10 pellet barrels (4 barrels with ΔN (total number of particle/ barrel) = 1×10^{21}, 3 with ΔN = 2×10^{21}, 3 with ΔN = 3×10^{21}) and continuous pellet injector (ΔN = 1×10^{21}, interval ≥ 100msec) [11]. Figure 2 shows how the injection of a series of pellets, each producing a spike on the H_α diagnostic, raises the density. The initial density profile is flat. At t = 0.78 s, the profile takes on a peaked shape. Subsequent pellets raise the density while retaining the peaked shape characteristic of SDC plasmas (Fig. 1). After t = 0.94 s, when the last pellet is injected, n(0) decays continuously with a time constant ~ 1 s , indicating that the diffusion coefficient in the IDB is less than 0.02 m^2s^{-1}. W_p decreases slightly and at t = 0.955 s, W_p starts to increase—the relative increase in temperature is greater than the simultaneous

decrease in density—and reaches its maximum value at t = 1.10 s. Similar behavior has been observed in a transient "reheat events" [12]. SDC plasmas, however, are maintained in a quasi-steady state by continued pellet injection [7].
The transport behaviors after injection of a single pellet are summarized as follows: the temperature drops adiabatically when the density is raised by an injected pellet. Sometimes it drops more, indicating deterioration of the transport. When the pellet size is too large, a radiative collapse occurs. The confinement deteriorates immediately after the pellet injection probably due to rapid change in density profile from peaked to broader edge density profile. When it becomes peaked again during the density decay phase, the confinement starts to improve, i.e., the "reheat event" starts. The stored thermal energy continues to increase for the order of the energy confinement time and reaches the maximum value and then decays

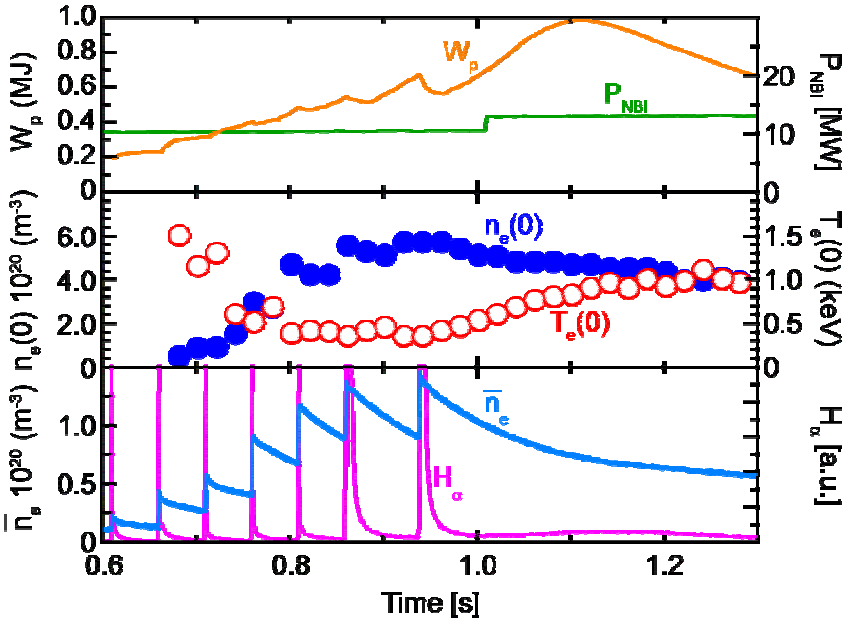

Fig. 2 Time evolution of the plasma parameters in the SDC plasma operation.

4. Comparison between SDC and gas puffed discharges

The function of the LID in the SDC formation is to pump edge-recycled particles thereby maintaining a low edge density. This results in high edge electron temperature gradients. During a sequence of many LID discharges, the wall conditioning take place and thus the wall pumping capability is enhanced. SDC plasmas with somewhat lower temperatures can then be obtained even without the LID. For longer pulse operation in the SDC mode, however, active pumping by the divertor is essential.
The advantage of the SDC discharge over the conventional discharge is easily shown by simply comparing two discharges, SDC LID discharge (Fig.1) and a gas puffed LID discharge with similar plasma conditions except for the density profiles shape (Fig.3(a)). For the gas puffed case, the density profile is flat because the particle source is localized in the very edge, even outside of the last closed magnetic surface. The plasma thermal energy density profiles (3nT) for both cases are plotted in Fig.3(b). In the outer region, the thermal energy density is nearly identical. The total thermal energy for the gas puff case is ~ 400 kJ and the total thermal energy in the core part (denoted by green color) of the SDC is ~600 kJ and this portion of the thermal energy is the gain of the SDC discharge over the gas puff discharges.

The SDC discharge exhibits the highest fusion plasma performance achieved so far on LHD, $n_o\tau_E T_o$ (fusion triple product) ~ 4.4×10^{19} keVm^{-3}s, despite a ~ 40 % reduction in effective confinement volume (due to the LID) from standard LHD discharges (helical divertor, B = 2.75 T, R_{ax} = 3.6 m). Note that in addition to τ_E enhancement, peaking of the thermal energy density profile also contributes to enhance the triple product. For the gas puffed discharge (Fig.3 (a)), the fusion triple product is ~ 0.32×10^{19} keVm^{-3}s, an order of magnitude lower compared with the SDC case.

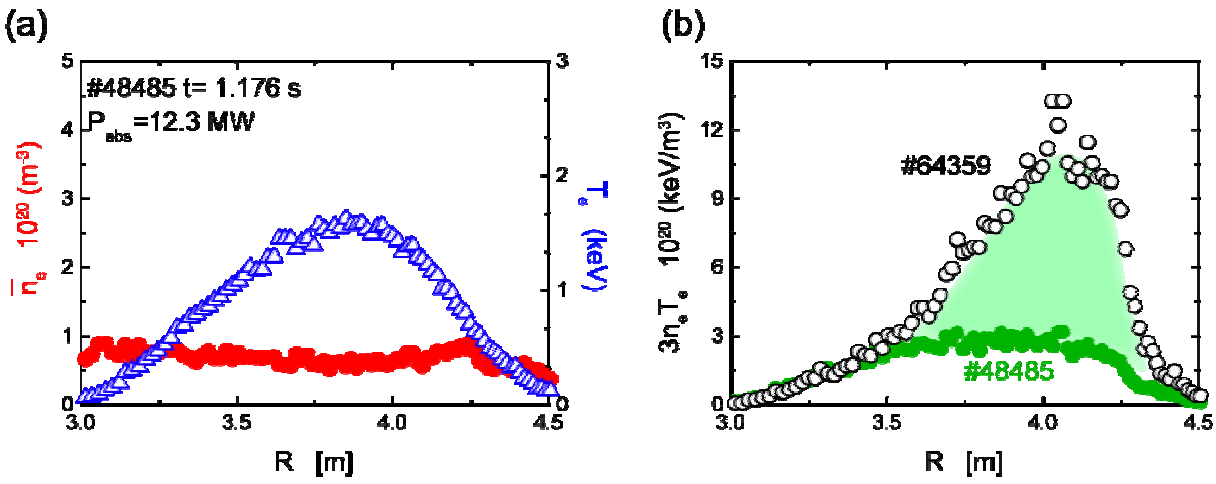

Fig. 3 Comparison between the SDC LID discharge and the gas puffed LID discharge. (a) Density and temperature profiles for gas puffed discharge. (b) Comparison of the thermal energy density between the SDC discharge and the gas puffed discharge.

5. Configuration dependence

The minor radial extent of the SDC is determined by the IDB foot location (jump in ∇n), and increases with R_{ax} and β. Figure 4(a) plots the observed plasma pressure (nT) profile and the calculated rotational transform (ι/2π) profiles as a function of ρ for the SDC configuration with R_{ax} = 3.75. In estimating the rotational transform, we use the equilibrium code, assuming that the pressure profile is expressed by P (ρ) = P (0) $(1-\rho^2)^2$, which is close to the observed profile. The IDB foot falls at ρ = 0.56. It is close to the zero radius (dι/dρ = 0) in the ι/2π profile. In the low beta cases, the shear is nearly zero in the core and thus the zero shear radius can not be defined. To avoid the confusion, R_{sp} is defined as the major radius of the intersection point of the lines of tangency to the inner and outer portions of the iota profile. As in Fig.4 (a), with enough negative shear in the inner region, it is nearly equal to R_{zs} [the zero shear radius (dι/dR = 0)]. Inside this radius (R_{sp}), the rotational transform profile has modest negative or nearly zero shear and a magnetic well. Outside this location, it has positive shear and a magnetic hill. Figure 4-b shows the observed major radii of the foot location, R_{foot} and calculated R_{sp} as a function of the average beta for three different configurations (R_{ax} = 3.65m, 3.75m, 3.85m). The IDB foot point falls close to R_{sp}.and the difference between R_{sp} and R_{foot} is found to be less than ~ 0.10 m. The foot point location is found to be more closer to boundary between the magnetic hill and well.

For fixed configuration magnetic axis position (R_{ax}), the zero-shear surface moves outward in ρ with increasing β. For a fixed value of β, the zero-shear radius also moves outward (increasing the volume of the core region) as R_{ax} is increased.

The "standard" configuration (R_{ax} = 3.75 m) with β(0) = 4.4 %, and the IDB foot at ρ = 0.56 yields an SDC with the optimum performance. For the outward shifted configuration (R_{ax} = 3.85 m), the SDC grows with increasing β and the IDB foot moves outward toward the last closed surface at <β> = 1.4 %. For the inward shifted case (R_{ax} = 3.65m), the SDC is smaller, with the IDB foot at ρ = 0.45 at <β> = 0.5%, corresponding to R_{foot} = 4.10 m in Fig. 4(b). While the overall shape of the density profile is similar to that of the optimum case, the "super dense" effect is weaker in our experiments so far.

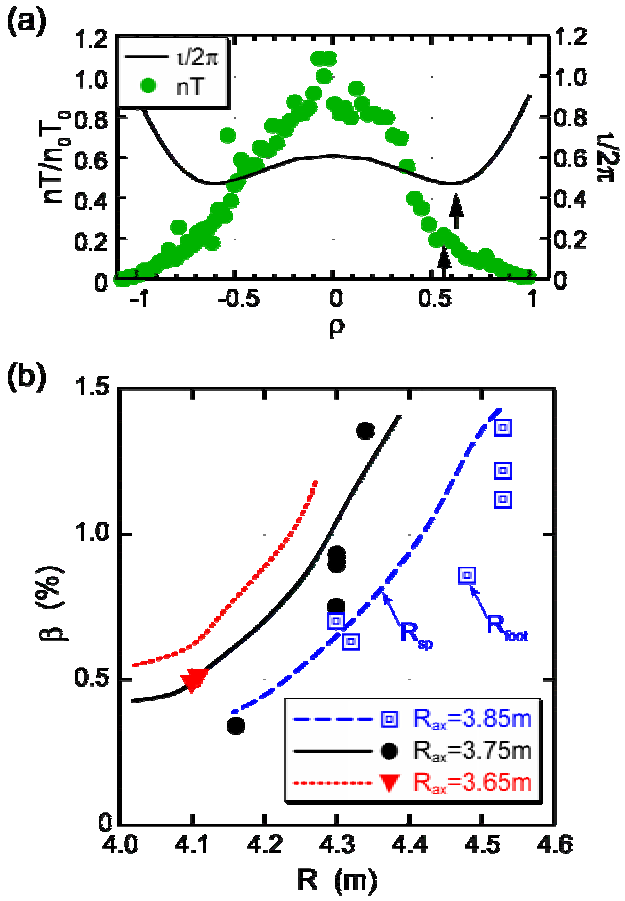

Fig. 4 (a) Typical pressure profile in SDC plasma operation. The location of the IDB foot is R_{foot} = 4.33 m (ρ=0.56). The location of zero shear R_{zs} = 4.39 m, (b) With increasing beta and R_{ax}, the foot location of the IDB (R_{foot}) increases. The blue, black and red curves are R_{zs} for R_{ax} = 3.85, 3.75, 3.65m, respectively.

6. Formation of high beta SDC by reheat event

In order to study the MHD properties of the SDC plasmas, we have made an attempt to achieve higher β at lower field (B = 1.5 T). The maximum β value so far is <β> = 1.4 % (β(0) = 5.1 %). We do not see any detrimental MHD activities such as a sawtooth crash or ELM, as seen in case of tokamak improvement modes [13-14]. The time evolution of the SDC plasma (see Figure 5-a) shows that the SDC forms at 0.6 s. During frequent pellet injection phase (0.6 s to 0.7 s), the density is raised, but increase in the stored plasma energy is somewhat suppressed. After terminating the pellet injection (t = 700 ms), the stored plasma energy and hence <β>

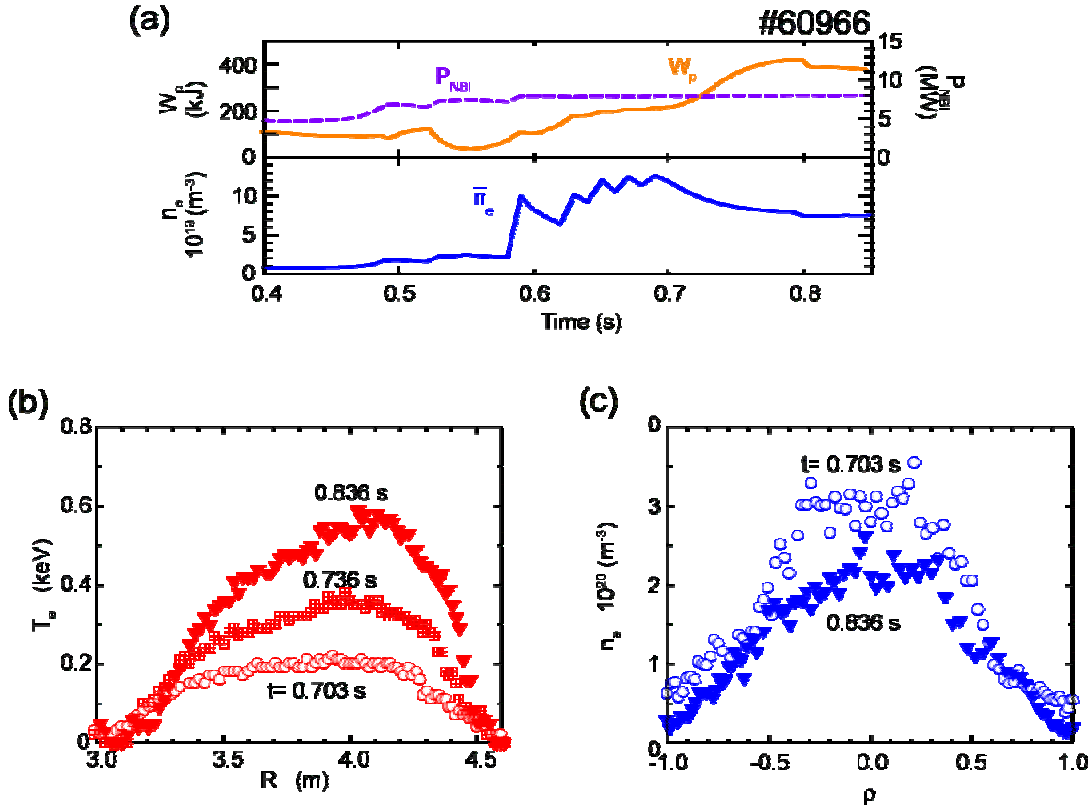

Fig. 5 (a) Time evolution of high β discharge with a "reheat" event from t= 700 ms. (b) Time evolution of the temperature profile (t= 703, 736, 836 ms). (c) The density profiles just before termination of the pellet injection (t= 703 ms). The profiles near the peak of the W_p (stored energy) (t= 836 ms).

increases for 0.1 s and reach the maximum. This SDC reheat event is very drastic. Fig. 5(b) shows a clear, significant change of the helical plasma equilibrium, i.e., the magnetic axis of the plasma moves outwards significantly (a large Shafranov shift). At t = 0.703 s, the temperature and density profiles are those of the typical SDC mode, shown in Fig. 5(b),(c). The temperature starts to increase except for the outer region (R > 4.45m, R<3.25 m) [Fig. 5(b)] and the profile at t = 0.736 s has a modest temperature gradient in the core and begins to deviate from the SDC type profile. Because of lower field, the central density decay rate is much higher without pellet core fueling and thus the central density decreases by 25 % at t = 0.836 s. During this evolution, the temperature nearly triples, exhibiting a significant improvement of the confinement. The temperature gradients both in the core and in outer region also increase, deviating from the typical SDC profile (flat core profile) when <β> exceeds 1%. What causes the above evolution remains unclear. We note that the density beyond ρ = 0.7 during the reheat phase is substantially lower than that at t = 0.703 s (during frequent pellet injection phase). Peaking in the edge density profile could lead to higher temperature in the outer region. Combined effects of the high density in the core (SDC effect) and high temperature in the outer region (reheat effect) leads to a significant confinement enhancement.

We have examined the ideal MHD stability of these configurations using the 3-D COBRA stability code [15]. We find that the core region inside the zero-shear radius has direct access

to second stability, i.e., the stability margin increases with β. Outside the zero shear radius, the plasma becomes unstable to ballooning modes at average β ~3-4%, which is a factor of 2 higher than the achieved value. Of course, resistive versions of the modes are expected to appear at lower β. These results suggest that MHD effects may play a role in improving core confinement, and may also provide a useful mechanism to constrain the plasma pressure in the outer region of the plasma, thus helping maintain the favorable SDC state.
Modes somewhat similar to SDC have been observed in the pellet fueled tokamak discharges [16, 17]. They appear when the shear in the core is reversed by the pellet fueling as in the LHD SDC. The main issue is the MHD stability, which result in a plasma collapse and thus not much attention has been paid to them.

7. Ignition scenario based on SDC concept

These results suggest a novel fusion ignition scenario in which an SDC is used to operate at very high density and relatively low temperature in the core and at low density in the outer region (note that low density helps to raise the temperature above the value required for reasonably high fusion reaction rate). Such a scheme is particularly attractive for helical devices because (a) they do not require current drive (which is ineffective at higher density), and (b) operation at high collisionality reduces the effect of the helical ripple diffusion regime. We propose the ignition scenario with lowest possible core temperature (7-8 keV), below which the fusion reaction rate decreases significantly. The core plasma pressure is determined by the core beta value imposed by MHD constraints. The fusion alpha power density is proportional to the square of the plasma pressure and thus lower core temperature can be compensated by higher core density. In the outer region, the low density is desirable, i) the temperature gradient there can be high, ii) radiative collapse can be avoided. The SDC density profile (high density core + low density edge) can be maintained by IDB with pellet fueling and divertor pumping.

8. Summary

A **S**uper **D**ense **C**ore (**SDC**) plasma operational regime has been discovered in Local Island Divertor discharges in which the core plasma is fuelled by pellet injection and the particles recycled at the divertor plates are pumped effectively. A core region with densities as high as $4.6\times10^{20}m^{-3}$ and temperatures of 0.85 keV is maintained by an internal diffusion barrier (**IDB**) with a very high density gradient.

This work is supported by NIFS05ULPP506.

References

[1] Motojima, O., et al., 1999 Phys. Plasmas **6** 1843.
[2] Wagner, F., et al., 1982 Phys. Rev. Lett. **49** 1408.
[3] Ohyabu, N., et al., 1999 J. Nucl. Mater. **266-269** 302.
[4] Komori, A., et al., 2004 Fusion Science and Technology **46** 167.
[5] Morisaki., T., et al., 2005 J. Nucl. Mater. **337-339** 154.
[6] Masuzaki, S., et al., 2006 To be submitted to Nucl. Mater..
[7] Ohyabu, N., et al., 2006 Phys. Rev. Lett. **97** 055002.
[8] Levinton, F. M., et al., 1995 Phys. Rev. Lett. **75** 4417.
[9] Strait, E. J. et al., 1995 Phys. Rev. Lett. **75** 4421.
[10] Fujita, T., et al., 1998 Nucl. Fusion **38** 207.

[11] Sakamoto, R., et al., 2001 Nuclear Fusion **41,** 381.
[12] Morita, S., et al., 1993 Proc. 14th International Conference on Plasma Physics and Controlled Nuclear Fusion Research Wurzburg 1992 IAEA-CN-56/C-2-5.
[13] Gohil, P., et al., 1988 Phys. Rev. Lett. **61** 1603.
[14] Zohm, H., et al., 1996 Plasma Phys. Control. Fusion **38** 105.
[15] Sanchez, R., et al., 2001 Comp. Phys. Comm **141** 55.
[16] Milora, S. L., et al., 1986 Plasma. Phys. Contol. Fusion **28** 1435.
[17] Smeulders,P., et al., 1995 Nucl. Fusion **35** 225.